Calcium-activated K^+ Channels of Mouse β-cells are Controlled by Both Store and Cytoplasmic Ca^{2+}: Experimental and Theoretical Studies

P.B. Goforth,[1] R. Bertram,[4] F.A. Khan,[3] M. Zhang,[1] A. Sherman,[5] and L.S. Satin[1,2,3]

[1]Departments of Pharmacology and Toxicology, [2]Physiology, and [3]Medicine (Endocrinology), Medical College of Virginia at Virginia Commonwealth University, Richmond, VA 2398

[4]Department of Mathematics and Kasha Laboratory of Biophysics, Florida State University, Tallahassee, FL 32306

[5]Mathematical Research Branch, National Institute of Diabetes and Digestive and Kidney Diseases, National Institutes of Health, Bethesda, MD 20892

ABSTRACT A novel calcium-dependent potassium current (K_{slow}) that slowly activates in response to a simulated islet burst was identified recently in mouse pancreatic β-cells (Göpel, S.O., T. Kanno, S. Barg, L. Eliasson, J. Galvanovskis, E. Renström, and P. Rorsman. 1999. *J. Gen. Physiol.* 114:759–769). K_{slow} activation may help terminate the cyclic bursts of Ca^{2+}-dependent action potentials that drive Ca^{2+} influx and insulin secretion in β-cells. Here, we report that when $[Ca^{2+}]_i$ handling was disrupted by blocking Ca^{2+} uptake into the ER with two separate agents reported to block the sarco/endoplasmic calcium ATPase (SERCA), thapsigargin (1–5 μM) or insulin (200 nM), K_{slow} was transiently potentiated and then inhibited. K_{slow} amplitude could also be inhibited by increasing extracellular glucose concentration from 5 to 10 mM. The biphasic modulation of K_{slow} by SERCA blockers could not be explained by a minimal mathematical model in which $[Ca^{2+}]_i$ is divided between two compartments, the cytosol and the ER, and K_{slow} activation mirrors changes in cytosolic calcium induced by the burst protocol. However, the experimental findings were reproduced by a model in which K_{slow} activation is mediated by a localized pool of $[Ca^{2+}]$ in a subspace located between the ER and the plasma membrane. In this model, the subspace $[Ca^{2+}]$ follows changes in cytosolic $[Ca^{2+}]$ but with a gradient that reflects Ca^{2+} efflux from the ER. Slow modulation of this gradient as the ER empties and fills may enhance the role of K_{slow} and $[Ca^{2+}]$ handling in influencing β-cell electrical activity and insulin secretion.

KEY WORDS: islets of Langerhans • KCa channels • ER • insulin • intracellular calcium

INTRODUCTION

β-Cells of the islets of Langerhans control blood glucose levels by secreting insulin in response to an increase in extracellular glucose. At glucose concentrations ≥7 mM, glucose metabolism triggers rhythmical electrical activity in mouse islets. This activity consists of periodic depolarizing plateaus with superimposed rapid spikes, separated by silent phases of −65 mV (Dean and Matthews, 1968, 1970; Meissner and Schmelz, 1974; Rosario et al., 1993; Satin and Smolen, 1994). Glucose-induced closure of ATP-dependent potassium (K_{ATP}) channels depolarizes islets to about −50 mV, where bursting commences. The spikes and plateaus are mediated by voltage-activated Ca^{2+} channels (Meissner and Schmeer, 1981; Ribalet and Beigelman, 1981) and increasing glucose increases calcium influx, $[Ca^{2+}]_i$, and insulin secretion by prolonging the spiking plateau phase and concomitantly shortening the silent phase (Cook, 1984). β-Cell electrical activity is tightly coupled to insulin secretion, since the spiking phase duration and the rate of insulin secretion have the same dependence on glucose concentration (Meissner and Schmelz, 1974; Wollheim and Sharp, 1981; Ashcroft and Rorsman, 1989).

Despite extensive investigation, the ionic basis of islet pacemaking is still incompletely understood. The cyclic activation of Ca^{2+}-activated K^+ (K_{Ca}) current has long been considered a candidate ionic pacemaker mechanism (Atwater et al., 1979; for reviews see Satin and Smolen, 1994; Sherman, 1996), since islet bursting is readily simulated by theoretical models that incorporate the activation and deactivation of K_{Ca} channels by bursting-induced $[Ca^{2+}]_i$ oscillations (i.e., Chay and Keizer, 1985). However, direct characterization of the rapidly activating, large conductance K_{Ca} channels of β-cells that were the first K_{Ca} channels identified in these cells (Cook et al., 1984) raised doubts that they constituted the primary pacemaker mechanism. In particular, charybdotoxin, a selective inhibitor of large conductance K_{Ca} channels, was reported to have no effect on islet electrical activity (Kukuljan et al., 1991), and the voltage dependence of these channels is incompatible with their mediating a sustained repolarization to −65 mV after each burst. In addition, studies using $[Ca^{2+}]$-

The online version of this article contains supplemental material.

Address correspondence to Leslie S. Satin, Department of Pharmacology and Toxicology, Medical College of Virginia Virginia Commonwealth University, P.O. Box 980524, Richmond, VA 23298. Fax: (804) 828-1532; E-mail: lsatin@hsc.vcu.edu

http://www.jgp.org/cgi/doi/10.1085/jgp.20028581

sensing fluorescent dyes to monitor temporal changes in $[Ca^{2+}]_i$ during islet bursting suggest that islet $[Ca^{2+}]_i$ rises rapidly to a steady-state plateau at the beginning of each burst (Santos et al., 1991). This observation would seem to be incompatible with models requiring that $[Ca^{2+}]_i$ accumulate slowly during each burst and gradually activate Ca^{2+}-dependent K^+ current to terminate the burst (for review see Satin and Smolen, 1994).

The recent report of a slowly activating K_{Ca} current (K_{slow}) observed in in situ β-cells has led to renewed interest in a K_{Ca}-dependent model of islet bursting (Göpel et al., 1999). Göpel et al. (1999) presented evidence that K_{slow} tracks $[Ca^{2+}]_i$ as it slowly rises in response to a voltage clamp command designed to mimic an islet burst. In contrast to the fast β-cell K_{Ca} channel (Kukuljan et al., 1991), K_{slow} was insensitive to charybdotoxin or low concentrations of TEA, and its conductance was voltage-independent between −80 and −40 mV (Göpel et al., 1999). Together, these properties make K_{slow} a more attractive candidate than the large conductance K_{Ca} channel for mediating islet pacemaking.

In this study, we examined whether agents known to alter the $[Ca^{2+}]_i$ dynamics of β-cells affect K_{slow}. Of special interest to us was the possibility that altering the Ca^{2+} filling state of the β-cell endoplasmic reticulum would alter K_{slow}. Recent reports suggested that thapsigargin (Tg),* a well-known blocker of the sarco/endoplasmic calcium ATPase (SERCA), partially suppresses K_{slow} in in situ β-cells (Göpel et al., 1999) and inhibits K^+ efflux through tolbutamide- and charybdotoxin-insensitive K^+ channels in islets (Hennige et al., 2000). Here we show that Tg has a biphasic effect on K_{slow}, consisting of transient potentiation followed by sustained inhibition of the channel. Further, we show that insulin, which has also been reported to block SERCA through insulin receptor phosphorylation of IRS-1 in β-cells (Xu et al., 1999), has the same biphasic effect on K_{slow} as Tg. These results can be accounted for by a novel model in which K_{slow} activation depends on the buildup of $[Ca^{2+}]$ in a restricted submembrane space between the ER and the plasma membrane of the β-cell. In contrast, a more simplified model of β-cell Ca^{2+} handling including an ER component but lacking the subspace is unable to duplicate our experimental findings. The subspace model is a variant of our recent Phantom Burster Model of islet bursting (Bertram et al., 2000), in which two slow negative feedback processes combine to produce a range of intermediate electrical oscillations. In addition to reproducing K_{slow} currents measured in voltage-clamp, the model also reproduces the electrical bursting we see in elevated glucose. Finally, the model accounts for the previously reported depolarizing effects of Tg on islet electrical activity (Worley et al., 1994a, Bertram et al., 1995) without recourse to store-operated (SOC or CRAC) currents.

Abbreviations used in this paper: CICR, Ca^{2+}-induced Ca^{2+} release; CPA, cyclopiazonic acid; PMCA, plasma membrane Ca^{2+}-ATPase; SERCA, sarco/endoplasmic reticulum calcium ATPase; TG, thapsigargin.

MATERIALS AND METHODS

Cell Culture

Pancreatic islets were isolated from male Swiss-Webster mice that were killed by cervical dislocation. The bile duct of the pancreas was cannulated and injected with collagenase (2 mg/ml) dissolved in Kreb's solution consisting of (in mM): 135 NaCl, 5 KCl, 1 $CaCl_2$, 1.2 $MgCl_2$, 10 HEPES, 5 $NaHCO_3$, 5 glucose, 1 mg/ml bovine serum albumin, and 1% penicillin-streptomycin, pH. 7.35. Alternatively, collagenase was dissolved in Kreb's and then injected directly into the pancreas. The pancreas was then removed, placed in a culture dish, and incubated at 37°C for 5–10 min until the exocrine tissue was digested. Collagenase digestion was stopped by the addition of cold Kreb's solution. Tissue was then washed, triturated using a Pasteur pipette, and centrifuged. Islets were picked and placed into fresh Kreb's solution cooled to 4°C. Islets were then picked a second time, transferred to culture dishes containing enriched RPMI-1640 culture medium, and incubated at 37°C for 2–4 d.

To produce dispersed β-cells, islets were placed in a Ca^{2+}-free solution containing 9.5 mg/ml Spinners salts, 3 mM EGTA, 16 mM glucose, 1 mg/ml bovine serum albumin, pH 7.35, incubated at 37°C for 3 min and triturated lightly until the islets were fully dispersed into single cells. The resulting cell suspension was then centrifuged for 5 min. Following removal of the supernatant, cells were washed with Kreb's solution, and centrifuged again for 5 min. The supernatant was removed and the dispersed cells were resuspended in enriched RPMI-1640 medium (as above) and then plated onto glass coverslips. Cells were kept at 37°C in an air/CO_2 incubator and fed every 2–3 d.

Electrophysiology

Glass coverslips containing dispersed β-cells were transferred to a recording chamber held at 35°C mounted on an Olympus IX70 inverted microscope. Intact islets were immobilized using a large diameter suction pipette (Göpel et al., 1999). Electrical activity and whole-cell currents were recorded using an Axopatch 200 B amplifier (Axon Instruments, Inc.) and the perforated patch technique (Falke et al., 1989). Patch electrodes were pulled from borosilicate glass capillaries (WPI) and their tips were filled with a solution containing (in mM) 76 K_2SO_4, 10 NaCl, 10 KCl, 1 $MgCl_2$, and 5 mM HEPES, pH 7.35. The pipettes were then backfilled with the same internal solution containing 0.3 mg/ml amphotericin B. Increased pipette-cell capacitance and decreased series resistance signaled successful perforation. Experiments commenced when a steady zero current potential was obtained, usually within 2–15 min of obtaining a gigaseal. The external recording solution contained (in mM): 140 NaCl, 3.6 KCl, 2 $NaHCO_3$, 0.5 NaH_2PO_4, 0.5 $MgSO_4$, 5 HEPES, pH 7.4. External solution was prewarmed to 35°C and the recording chamber was perfused at a rate of 2.5 ml/min. Data were filtered at 1 kHz and digitized at 2–5 kHz using a Macintosh G4 computer (Apple Computer) equipped with an Instrutech ITC-16 interface (Instrutech) and Pulse Control (Herrington and Bookman, 1994) and Igor Pro software (Wavemetrics). To identify β-cells in situ, only cells that displayed rhythmic bursting activity in the presence of 10 mM glucose were selected for study. Single cell capacitance was calculated by integrating the transient current response to a small hyperpolarizing voltage step. In the voltage

clamp mode, cells were clamped to a standard holding potential of −65 mV. K_{slow} current was assayed using a simulated pulse burst protocol similar to that used by Göpel et al. (1999). This protocol consisted of a 5-s depolarizing step from −65 to −40 mV followed by either a train of 26 voltage ramps, each lasting 200 ms, from −40 to 0 mV and back to −40 mV or by a train of 26 voltage steps from −40 to 0 mV, each lasting 150 ms with a 50-ms interval in between each step (Fig. 2 A). The train of depolarizations was followed by a step back to −40 mV for 10 s before the membrane potential was returned to −65 mV. In experiments where voltage-gated Ca^{2+} current was studied, current was measured in whole-cell mode in response to a series of 200-ms voltage steps from −65 to 10 mV applied at 0.2 Hz. To isolate Ca^{2+} current, Na^+ and K^+ currents were blocked by the addition of TTX (0.5 μM) and TEA (20 mM), respectively, to the extracellular solution, and CsCl substituted for K_2SO_4 in the patch pipette solution. Tg and cyclopiazonic acid were prepared as stock solutions in DMSO and insulin and apamin were prepared as stock solutions in water. All stocks were diluted 1:1,000 to 1: 5,000 for experiments. Cytochrome C was added to control and drug solutions when insulin or apamin were used.

Data Analysis

Statistical analysis was performed using Microsoft Excel for Macintosh or GraphPad Prism 2.0. Data are expressed as mean ± SEM. Significance was determined using Student's *t* tests or ANOVA.

Modeling

To test the hypothesis that K_{slow} is activated by Ca^{2+} that is released from the ER and accumulates in a small submembrane compartment, we constructed a mathematical model. Our main goal was to determine if such a model could account for the biphasic response of K_{slow} to SERCA inhibition. Additionally, we used the model to explore what role such a Ca^{2+}-activated K^+ current could play in mediating the oscillatory electrical activity that is characteristic of islets.

As in other β-cell models, we started with a current balance equation that determines the membrane potential, *V*,

$$C_m dV/dt = -I_{Ca} - I_{Kv} - I_{KCa} - I_{KATP} - I_{Leak}. \quad (1)$$

The relatively fast voltage-dependent Ca^{2+} current I_{Ca} and delayed rectifying K^+ current I_{Kv} mediate the fast spiking of the active phase; I_{KCa} is the Ca^{2+}-activated K^+ current corresponding to K_{slow}; and I_{KATP} is the ATP-dependent K^+ current. To isolate the rhythmogenic potential of K_{slow}, I_{KATP} was modeled as a current having a constant conductance. We describe the dependence of I_{KCa} on Ca^{2+} by a steep Hill function,

$$I_{KCa} = g_{KCa}[Ca^{2+}]^q/([Ca^{2+}]^q + K_d^q)(V - V_K). \quad (2)$$

A complete list of parameter values and details of the remaining ionic currents, which are similar to those in previous models, are available at http://www.jgp.org/cgi/content/full/jgp.20028581/DC1. The main emphasis here is on the compartmentalization of Ca^{2+} into intracellular pools. We first considered the simplest model (Model I) that could conceivably simulate the effects of SERCA inhibition. This model consisted of two compartments, the cytosol and the ER, with their Ca^{2+} concentrations denoted *c* and c_{ER}, respectively,

$$dc/dt = f_{CYT}(J_{IN} - J_{PMCA} - J_{SERCA} + J_{RELEASE}) \quad (3)$$

$$dc_{ER}/dt = f_{ER}(V_{CYT}/V_{ER})(J_{SERCA} - J_{RELEASE}). \quad (4)$$

The Js are fluxes into the cell through plasma membrane Ca^{2+} channels (J_{IN}), out of the cell through the plasma-membrane Ca^{2+}-ATPase (J_{PMCA}), from the cytosol to the ER through the SERCA pump (J_{SERCA}), and from the ER to the cytosol through ER Ca^{2+} channels ($J_{RELEASE}$). Ca^{2+} efflux mediated by the plasma membrane Ca^{2+}-ATPase (PMCA) takes the form $J_{PMCA} = k_{PMCA}\, c$, whereas the SERCA pump flux is $J_{SERCA} = k_{SERCA}\, c$. The plasma membrane influx is related to the Ca^{2+} current by $J_{IN} = -\alpha\, I_{Ca}$, where α is a proportionality constant that converts Ca^{2+} current to Ca^{2+} flux. Ca^{2+} efflux corresponding to Ca^{2+} release from the ER was taken to be proportional to the Ca^{2+} concentration gradient between the ER and the cytosol,

$$J_{RELEASE} = p_{ER}(c_{ER} - c). \quad (5)$$

$J_{RELEASE}$ could represent flux mediated by either inositol 1,4,5 trisphospate (IP_3) or ryanodine (RyR) receptors (Ämmala et al., 1991; Barker et al., 1994; Gromada et al., 1996; Liu et al., 1996; Islam et al., 1998); our model does not require that the detailed properties of these specific channel mechanisms be taken into account. The ratio of cytosolic to ER volume, V_{CYT}/V_{ER}, incorporates the differential effects of Ca^{2+} uptake and release on the ER and cytosol due to differences in their respective volumes.

As will be shown in the RESULTS section, this simple model could not account for the inhibition of K_{slow} after SERCA inhibition. One way to resolve this discrepancy is to add regenerative Ca^{2+}-induced Ca^{2+} release (CICR) to the model. Such a model can indeed account for the biphasic response of K_{slow} to thapsigargin, because the loss of CICR when stores are depleted results in lower levels of $[Ca^{2+}]_i$. However, previously published experimental data show that depolarization-induced $[Ca^{2+}]_i$ elevations are increased and not decreased by thapsigargin (Liu et al., 1995; Miura et al., 1997; Gilon et al., 1999; Arredouani et al., 2002).

Thus, we rejected the CICR model and considered an alternative. We added a third pool to the model, a submembrane compartment (referred to as the subspace for brevity) having concentration denoted c_{SS}. We refer to this version as Model II. In this case, *c* represents $[Ca^{2+}]$ in a bulk cytoplasmic compartment, which is distinct from a more restricted subspace and is referred to as just the cytosol for brevity. In this model, Ca^{2+} that passively enters the cell through plasmalemmal Ca^{2+} channels is actively sequestered into the ER via SERCA and then leaks out of the ER to increase c_{SS}. The subspace in turn passively exchanges Ca^{2+} with the cytosol, whence it is pumped out of the cell. See the diagram in Fig. 1. Although flux from the cytosol to the subspace can occur, release of Ca^{2+} from the ER maintains a standing gradient between the ER and the cytosol, which tends to drive Ca^{2+} from the subspace to the cytosol. As long as the ER is replete, subspace $[Ca^{2+}]$ will be greater than bulk cytosolic $[Ca^{2+}]$. We further postulate that this elevated fraction of Ca^{2+} is essential for K_{slow} activation. The corresponding equations for Model II are:

$$dc/dt = f_{CYT}(J_{IN} - J_{PMCA} - J_{SERCA} + J_X) \quad (6)$$

$$dc_{ER}/dt = f_{ER}([V_{CYT}/V_{ER}]J_{SERCA} - J_{RELEASE}) \quad (7)$$

$$dc_{SS}/dt = f_{SS}([V_{ER}/V_{SS}]J_{RELEASE} - V_{CYT}/V_{SS}J_X). \quad (8)$$

J_{IN}, J_{PMCA}, and J_{SERCA} are the same as in Model I, but Ca^{2+}efflux from the ER is now proportional to the Ca^{2+} concentration gradient between the ER and the subspace rather than the bulk cytosol,

$$J_{RELEASE} = p_{ER}(c_{ER} - c_{SS}), \quad (9)$$

and the exchange flux between subspace and cytosol is proportional to the concentration gradient between those two compartments,

$$J_X = p_X(c_{SS} - c). \quad (10)$$

The volume ratios again take into account the differential effect of each of the fluxes due to differences in the volumes of the communicating compartments, and now include the volume of the subspace, V_{SS}. The numerical values we used were V_{CYT}/V_{ER} = 25.0 and V_{CYT}/V_{SS} = 2.5. Note that in the model, the subspace is not microscopically small—it merely needs to be small enough to generate about a twofold Ca^{2+} concentration gradient between the subspace and the cytosol.

In the absence of quantitative details of these compartments, we made the model as simple as possible, while still consistent with the observed integrated behavior of the β-cells under varying conditions. These include both voltage clamp and free running conditions, and the presence and absence of SERCA inhibitors. For example, we have not included SERCA and PMCA pumps in the subspace compartment since they are not needed, but these could be included, provided they are not so strong as to destroy the concentration gradient between the subspace and the cytosol. Similarly, some degree of Ca^{2+} release from the ER directly to the cytosol can be accommodated, but in excess would flatten the subspace-cytosol gradient. Finally, p_{ER} could have been formulated as a Ca^{2+}-dependent parameter to incorporate some degree of CICR in the model. However, we omitted it to make clear that this added complexity is not needed to explain the data.

Model equations were integrated using standard numerical methods as implemented in the public domain program XPP (http://www.math.pitt.edu/~bard/xpp/xpp.html) running under Linux (XPP is also available for Windows). Visualization and graphical analysis were performed using XPP or XMGR for Linux (http://plasma-gate.weizmann.ac.il/Xmgr).

Online Supplemental Material

List of parameter values and details of ionic currents are available at http://www.jgb.org/cgi/content/full/jgp.20028581/DC1.

RESULTS

K_{slow} Is Modulated by SERCA Inhibitors

Because it has been reported that K_{slow} is Ca^{2+} dependent (Göpel et al., 1999), we investigated the effect of agents that are known to alter $[Ca^{2+}]_i$ on K_{slow} current. We first examined the effect of Tg, a SERCA pump inhibitor, which reduces Ca^{2+} influx into the ER, ultimately resulting in depletion of the ER Ca^{2+} store (Thastrup et al., 1990; Islam et al., 1992). Using the perforated patch technique (Falke et al., 1989), isolated β-cells were voltage clamped to a holding potential of −65 mV and ionic current was measured in response to a voltage command that simulated an islet burst (see MATERIALS AND METHODS). Application of this voltage protocol elicited a slowly activating outward current that closely resembled K_{slow}, as described previously (Göpel et al., 1999). Fig. 2 A shows the total current (top trace) elicited by the simulated burst protocol (bottom trace) in a single dispersed mouse β-cell. Stepping membrane potential from −65 to −40 mV produced a small net increase in outward current in most cells (arrow 1). The subsequent 5-Hz train of membrane depolarizations from −40 to 0 mV activated transient outward currents during each pulse of the train (arrow 2). K_{slow} activation was manifested as a slow in-

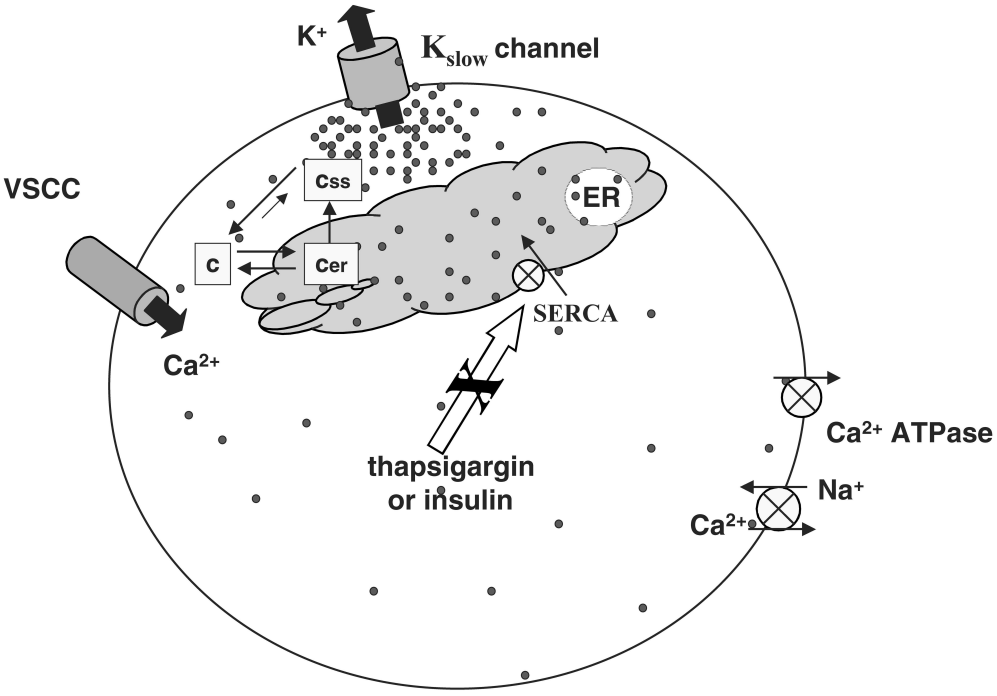

FIGURE 1. Model of K_{slow} activation by a localized ER-dependent gradient of calcium. Ca^{2+} entering the β-cell through voltage-sensitive Ca^{2+} channels is either extruded by the plasmalemmal Ca^{2+} ATPase or by Na^+/Ca^{2+} exchange or actively sequestered into the ER by SERCA. ER Ca^{2+} (c_{ER}) exits the organelle via Ca^{2+} channels that are in close proximity to K_{slow} channels, resulting in a local gradient of calcium c_{SS}, in the subspace. Subspace calcium is passively exchanged with cytosolic calcium, c. Thapsigargin or insulin block the uptake of calcium into the ER via SERCA.

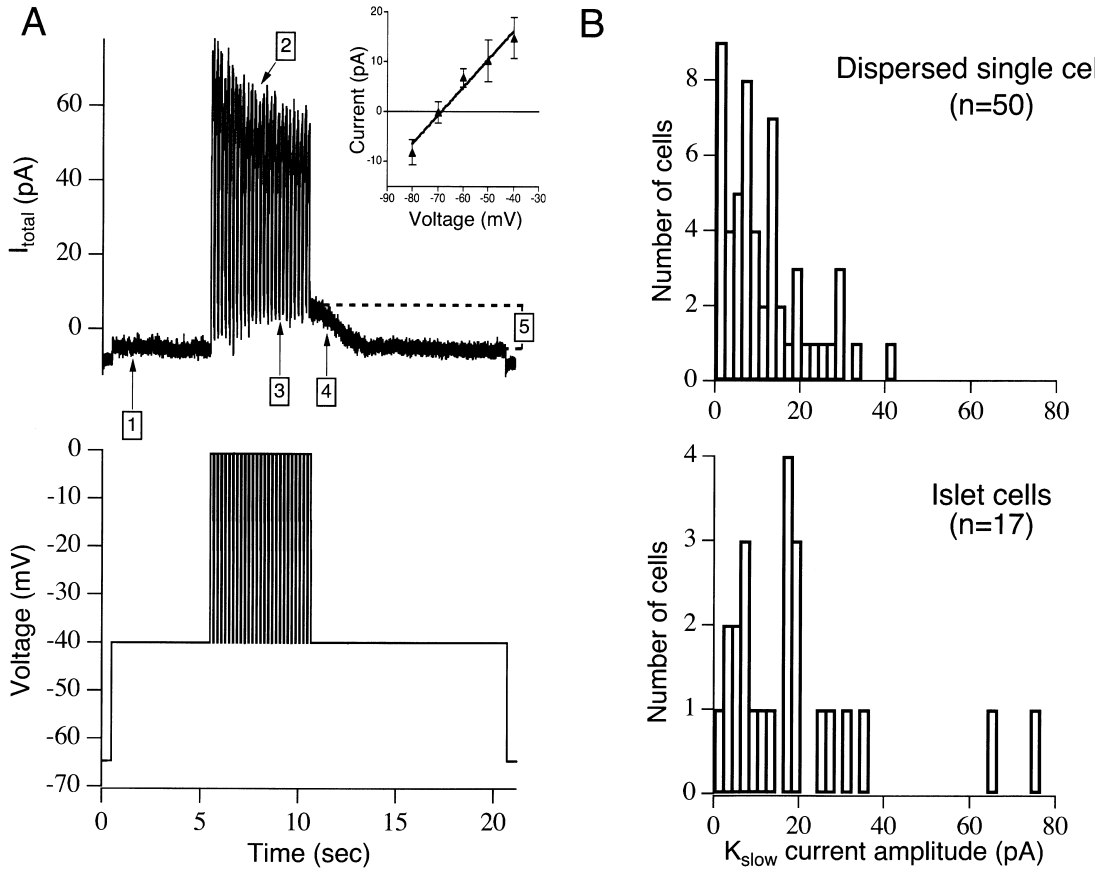

FIGURE 2. A simulated burst voltage command elicited a robust K_{slow} current in dispersed β-cells. (A) Total current (top trace) recorded from a single dispersed β-cell in response to a voltage-clamp command that simulated an islet burst (bottom trace). (1) Net outward current elicited by the initial step from −65 to −40 mV; (2) transient outward currents elicited by the train of depolarizations from −40 to 0 mV; (3) K_{slow} current measured at −40 mV gradually increased during the pulse train; (4) K_{slow} current gradually declined following the termination of the pulse train; (5) K_{slow} current amplitude was measured as the difference between the maximal current activated at −40 mV during the pulse train and the steady-state current measured at −40 mV following the pulse train. (Inset) I-V relationship for K_{slow} current measured at the end of the pulse train ($n = 3$). (B) K_{slow} amplitude histograms for a population of dispersed β-cells (top) and in situ β-cells (bottom).

crease in outward holding current at −40 mV, which typically continued for the duration of the burst (arrow 3). Upon cessation of the pulse train, the slowly activating outward current gradually decreased as K_{slow} deactivated (arrow 4). K_{slow} amplitude was measured as the difference between the maximal "tail" current at the end of the train of fast depolarizations and the steady-state current at −40 mV after the burst (arrow 5).

Dispersed β-cells possessed robust K_{slow} current having a mean amplitude of 10.8 ± 1.4 pA ($n = 51$) that exhibited the same pharmacological properties and current-voltage (I-V) relationship reported previously by Göpel et al. (1999). Thus, the tail of K_{slow} current measured at the end of the pulse train reversed at −69 mV (inset, Fig. 2 A) and was completely blocked by the Ca^{2+} channel blockers nimodipine (10 μM) or $CdCl_2$ (200 μM); or intracellular Cs^+, which blocks K^+ channels. The current was partially blocked (48%) by 20 mM TEA, and was insensitive to 100 nM charybdotoxin or 1 μM apamin (unpublished data). Although similar to Göpel et al. (1999), the pharmacological properties of the K_{slow} current in the present study differ slightly from an apamin-insensitive K_{Ca} channel found in murine βTC-3 cells, which is inhibited by 100 nM charybdotoxin (Kozak et al., 1998). In contrast to Göpel et al. (1999), who reported that dispersed β-cells possessed much smaller K_{slow} current than in situ β-cells, we found that the amplitudes of K_{slow} currents measured from dispersed and in situ β-cells exhibited significant overlap (Fig. 2 B).

The application of 5 μM Tg to dispersed β-cells resulted in the biphasic modulation of K_{slow} current (Fig. 3). Thus, in 10 of 13 cells tested, the addition of Tg transiently increased K_{slow} amplitude within 3 min, and continued Tg exposure nearly completely suppressed K_{slow} within 5–15 min (Fig. 3, A and B). In 3 of 13 cells, we found that Tg suppressed K_{slow} current without exhibiting the initial potentiation phase. After Tg treat-

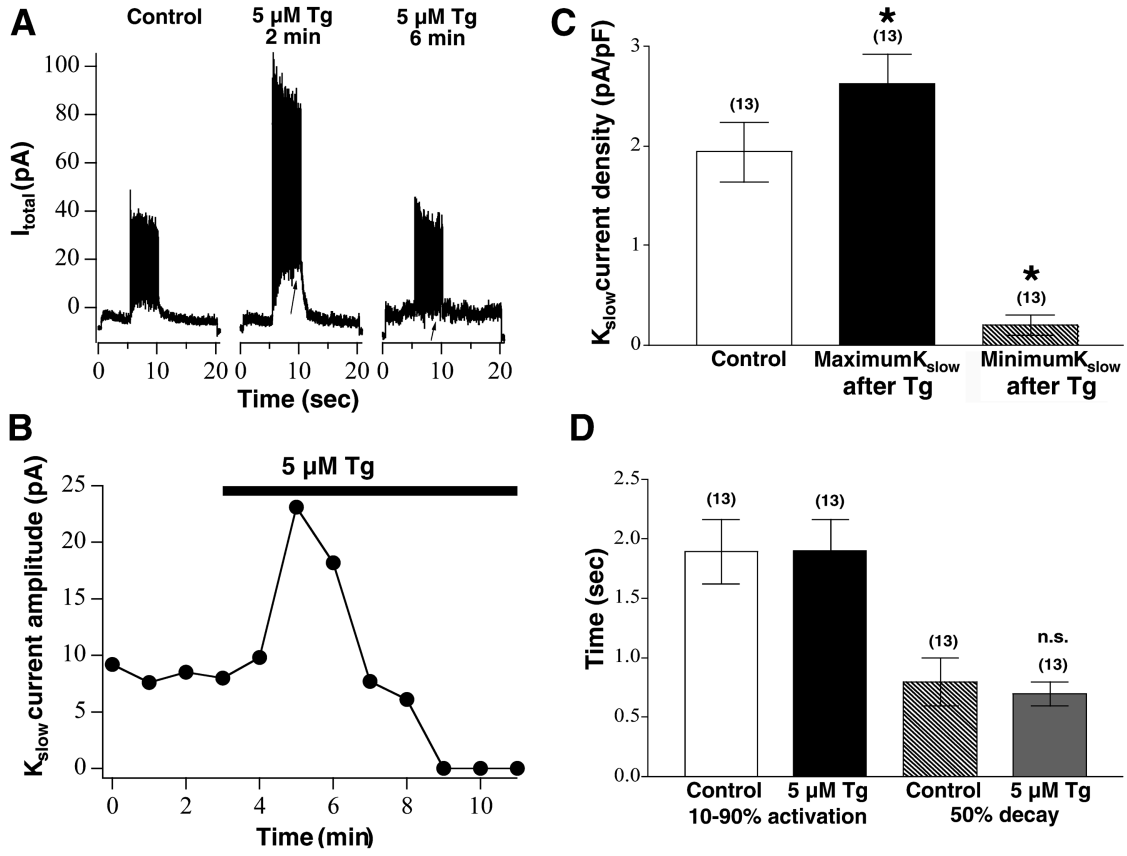

FIGURE 3. Thapsigargin modulates K_{slow} in a biphasic manner. (A) Total current recorded from a dispersed β-cell in response to a simulated burst command before (left trace) and during the application of 5 μM Tg. Tg transiently potentiated (middle trace) then suppressed (right trace) K_{slow} amplitude. (B) Time course of Tg-induced modulation of K_{slow} amplitude for the same β-cell. (C) After Tg application, mean K_{slow} current density increased from 1.9 ± 0.3 pA/pF to 2.6 ± 0.3 pA/pF then decreased to 0.2 ± 0.1 pA/pF (n = 13, P < 0.05 by ANOVA). (D) Tg did not affect the 10–90% rise time of K_{slow} during the pulse train or the time for K_{slow} to decay by 50% after the pulse train (n = 13, P > 0.05 by Student's t test).

ment, the mean K_{slow} current density for all cells rose significantly from 1.9 ± 0.3 pA/pF to 2.6 ± 0.3 pA/pF, and then decreased to 0.2 ± 0.1pA/pF (n = 13, P < 0.05) (Fig. 3 C). This is in contrast to a preliminary report that Tg only partly reduces K_{slow} in in situ β-cells (Göpel et al., 1999, 2001). The changes in K_{slow} amplitude we observed were not accompanied by changes in the activation or decay rate of K_{slow} (Fig. 3 D). The mean time for 10–90% activation of K_{slow} current was 1.8 ± 0.3 versus 1.9 ± 0.3 s (n = 13; P > 0.05) before and after Tg treatment, respectively, whereas the mean 50% decay time was 0.8 ± 0.2 versus 0.7 ± 0.1 s (n = 13; P > 0.05), for control and Tg treatment, respectively. Changes in K_{slow} amplitude produced by Tg were not due to current rundown or drift since control experiments showed that the current amplitude was stable over the length of the experiments (unpublished data). We also considered whether K_{slow} potentiation might be secondary to an increase in $[Ca^{2+}]_i$ due to the activation of CRAC channels (Worley et al., 1994a,b; Liu and Gylfe, 1997; Roe et al., 1998). Although Tg application did result in an increase in the inward holding current at −65 mV or the step in current resulting from changing V from −65 to −40 mV in some cells (unpublished data), these changes were not statistically significant. Thus, it is unlikely that CRAC activation accounts for the large changes we observed in K_{slow} after Tg treatment.

Similar results were obtained with the application of 1 μM Tg or 50 μM cyclopiazonic acid (CPA). The lower dose of Tg transiently increased then inhibited K_{slow} in one of six cells and inhibited K_{slow} without potentiation in five of six cells. This effect was irreversible. Likewise, CPA, a reversible SERCA inhibitor, transiently increased then inhibited K_{slow} in two of four cells and only inhibited K_{slow} in the remaining two cells. The effects of CPA were reversible.

The application of 1 μM Tg to unclamped dispersed β-cells resulted in an initial hyperpolarization then depolarization of membrane potential and could increase fast spiking (n = 4), consistent with previous reports (Worley et al., 1994a; Bertram et al., 1995; Gilon et al., 1999).

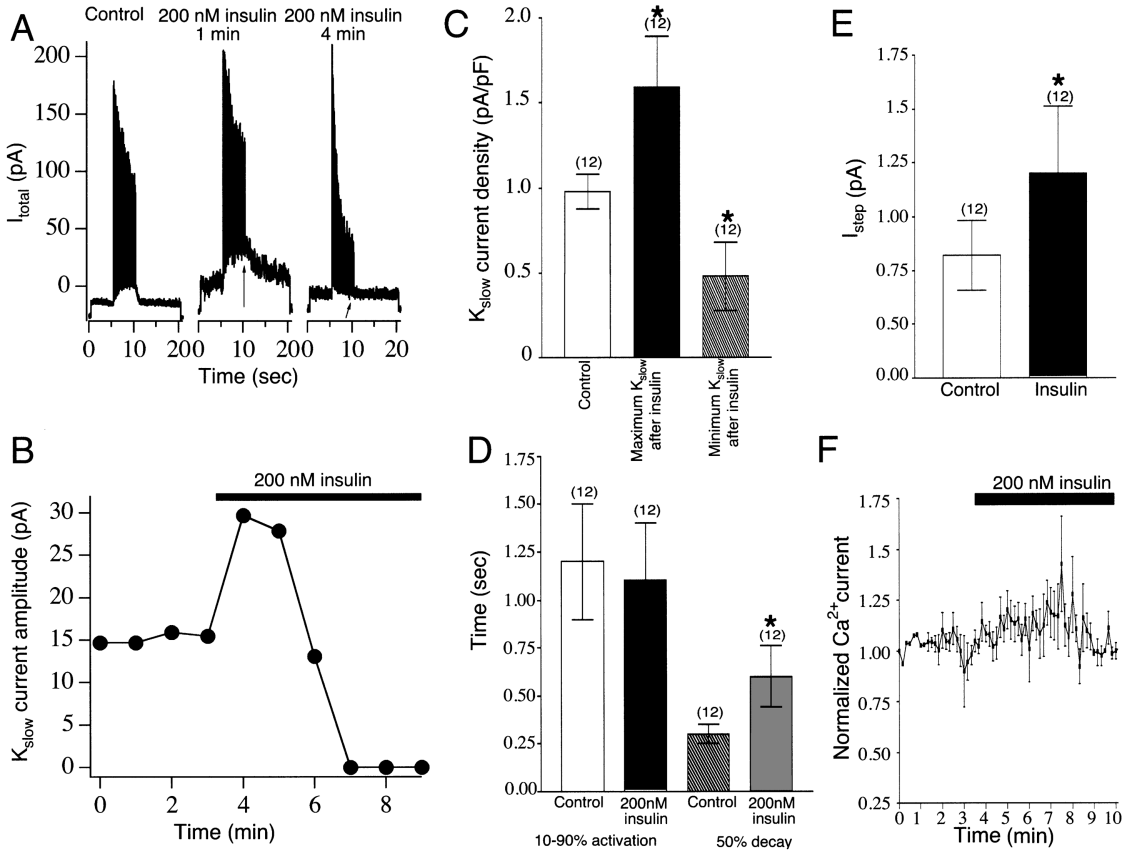

FIGURE 4. Insulin mimics the biphasic modulation of K_{slow} observed with Tg. (A) Total current recorded from a dispersed β-cell in response to a simulated burst command before (left trace) and during the application of 200 nM insulin. Insulin transiently potentiated (middle trace) then suppressed (right trace) K_{slow} amplitude. (B) Time course of insulin-induced modulation of K_{slow} amplitude for the same β-cell. (C) Following insulin application, mean K_{slow} current density increased from 1.0 ± 0.1 pA/pF to 1.6 ± 0.3 pA/pF then decreased to 0.5 ± 0.2 pA/pF (n = 12, P < 0.05 by ANOVA). (D) Insulin did not affect the 10–90% rise time of K_{slow} during the pulse train (n = 12, P >0.05 by Student's t test) but did slow the 50% decay time K_{slow} from 0.3 ± 0.1 s to 0.6 ± 0.2 s (n = 12, P < 0.05 by Student's t test). (E) Insulin increased the current elicited by the initial voltage step from −65 to −40 mV during the simulated burst command, from 5.6 ± 1.6 pA to 9.5 ± 3.1 pA (n = 12, P < 0.05 by Student's t test). (F) Application of 200 nM insulin did not significantly affect voltage-gated Ca^{2+} current measured in response to a series of 200 ms voltage steps from −65 to 10 mV given over the same experimental time course.

It has been shown recently that insulin activation of β-cell insulin receptors increases $[Ca^{2+}]_i$ by inhibiting SERCA via an IRS-1–dependent pathway (Xu et al., 1999). Therefore, we tested the hypothesis that insulin inhibition of β-cell SERCA would modulate K_{slow} similarly to Tg. We found that the application of 200 nM insulin to dispersed β-cells produced effects that indeed closely resembled those observed with Tg (Fig. 4). Thus, in 10 of 12 cells tested, exogenous insulin increased K_{slow} current amplitude within 2 min, and continued insulin exposure suppressed K_{slow} within 5 min (Fig. 4 B). Insulin increased the mean K_{slow} current density of all cells from 1.0 ± 0.1 pA/pF to 1.6 ± 0.3 pA/pF, followed by a reduction to 0.5 ± 0.2 pA/pF (n = 12; P < 0.05) (Fig. 4 C). As we found with Tg, insulin did not change the 10–90% activation rate of K_{slow}, which was 1.2 ± 0.3 versus 1.1 ± 0.3 s (n = 12; P > 0.05) for control and insulin treatment, respectively. However, K_{slow} decayed more slowly in the presence of insulin (Fig. 4 D), such that the mean time for 50% decay of K_{slow} increased from 0.3 ± 0.1 to 0.6 ± 0.2 s (n = 12; P < 0.05). Insulin exposure did not significantly change the amplitude of inward holding current at −65 mV. However, insulin did increase the size of the step current evoked by changing membrane potential from −65 to −40 mV. This current increased from 5.6 ± 1.6 to 9.5 ± 3.1 pA (n = 12, P < 0.05), consistent with our recently reported finding that insulin activates K_{ATP} channels in mouse β-cells (Khan et al., 2001) (Fig. 4 E).

Because it had been reported that insulin can augment L-type Ca^{2+} channel current in isolated rat ventricular myocytes (Aulbach et al., 1999), we considered whether the transient increase in K_{slow} current amplitude we observed might be secondary to an insulin-

induced increase in Ca^{2+} influx through voltage-sensitive Ca^{2+} channels. Therefore, we examined the effect of insulin on the voltage-sensitive Ca^{2+} currents of β-cells in a parallel study. As shown in Fig. 4 F, insulin did not significantly alter β-cell Ca^{2+} current, suggesting that K_{slow} potentiation does not appear to be due to the potentiation of β-cell Ca^{2+} channels.

Our finding that the depletion of ER Ca^{2+} stores by SERCA inhibitors modulates K_{slow}, ultimately leading to its suppression, is consistent with the hypothesis that ER Ca^{2+} stores are involved in the activation and regulation of K_{slow} current in β-cells. Since the long-term consequence of Tg exposure is to deplete the ER of Ca^{2+}, this suggests that filling of the β-cell Ca^{2+} stores is required for K_{slow} activation. This hypothesis was developed further by constructing a mathematical model of β-cell Ca^{2+} handling (see below).

Modulation of K_{slow} by Glucose

We next examined the sensitivity of K_{slow} to changes in extracellular glucose, which may alter intracellular Ca^{2+} handling by changing the energetics of the β-cell, since plasmalemmal Ca-ATPases and SERCA consume ATP. In dispersed β-cells, raising extracellular glucose from 5 to 10 mM shifted the holding current at −65 mV in the inward direction, from −5.2 ± 1.9 pA to −10.9 ± 2.6 pA ($n = 8$, $P < 0.05$), which would be expected for glucose-induced closure of K_{ATP} channels after a rise in ATP/ADP (Cook and Hales, 1984; Rorsman and Trube, 1985). In contrast to Göpel et al. (1999, 2001), we found that raising extracellular glucose reduced K_{slow} current density more than twofold, from 4.7 ± 1.3 to 2.2 ± 0.8 pA/pF ($n = 8$, $P < 0.01$) (Fig. 5).

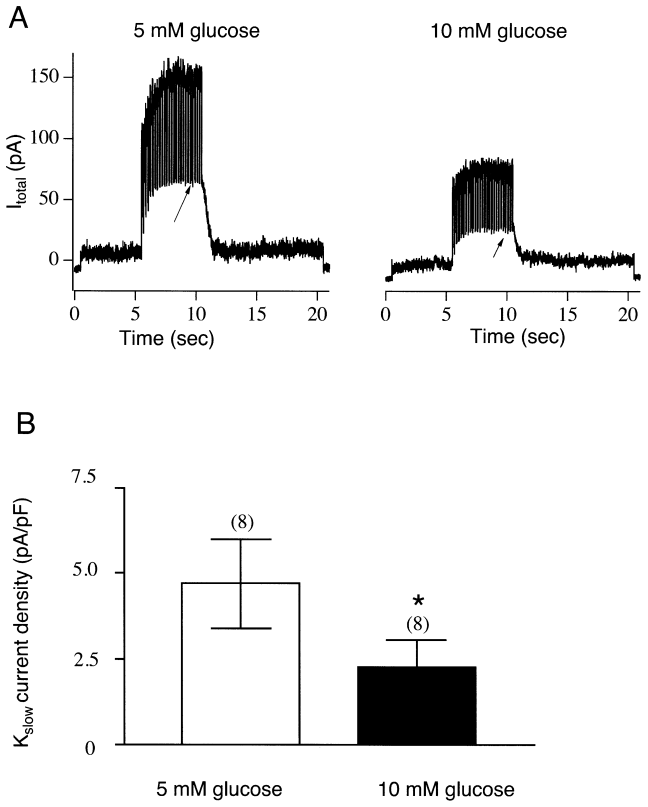

FIGURE 5. Raising extracellular glucose reduced K_{slow} amplitude. (A) Total current recorded from a dispersed β-cell in response to a simulated burst command in the presence of 5 mM (left trace) and 10 mM (right trace) glucose. Note the reduction of K_{slow} activation at −40 mV during the pulse train (arrow). (B) Mean K_{slow} current density decreased from 4.7 ±1.3 pA/pF to 2.2 ± 0.8 pA/pF ($n = 8$, $P < 0.01$ by Student's t test) in the presence of 5 or 10 mM glucose, respectively.

One possible explanation for the inhibitory effect of glucose on K_{slow} is that the net current measured at the end of the pulse train is actually an aggregate of K_{slow} and K_{ATP} channel currents, as has been suggested recently (Göpel et al., 2001). To determine whether this is the case, we tested the sensitivity of K_{slow} to tolbutamide, a specific blocker of K_{ATP} channels. The application of 100 μM tolbutamide to dispersed β-cells shifted the holding current measured at −65 mV from −10.8 ± 2.2 pA to −16.2 ± 3.6 pA ($n = 4$, $P > 0.05$), and reduced the current step elicited by the step from −65 to −40 mV, from 10.5 ± 5.8 pA to 5.8 ± 2.4 pA ($n = 4$, $P > 0.05$). More importantly, tolbutamide was without significant effect on K_{slow} amplitude, which was 11.2 ± 1.7 pA and 9.0 ± 0.6 pA ($n = 4$, $P > 0.05$), before and after the application of tolbutamide, respectively. This result stands in contrast with the 75% suppression reported in in situ mouse β-cells by Göpel et al. (2001). Thus, it appears that, in our hands, K_{ATP} channels do not significantly contribute to the total K_{slow} current in dispersed mouse β-cells. In addition, the enhanced current amplitude observed for K_{slow} in 5 mM glucose (relative to that in 10 mM glucose) persisted despite the presence of 100 μM tolbutamide (two of two cells), confirming that the glucose sensitivity of K_{slow} is unlikely to be due to the contamination of K_{slow} by K_{ATP} channels (unpublished data).

Modulation of K_{slow} by SERCA Inhibitors Can be Modeled by the ER-dependent Buildup of Ca^{2+} in a Submembrane Space

The earliest β-cell models considered only a single Ca^{2+} compartment, the cytosol. Obviously, such models cannot account for the effects of Tg and insulin that we observed—at minimum it is necessary to include the ER. Simulations demonstrate, however, that simply adding a conventional ER component is not sufficient to explain the biphasic effects of SERCA inhibitors in β-cells. Thus, Fig. 6 shows the result of applying the same protocol used in the experiments (Fig. 2) to a model cell incorporating an ER and a cytosolic compartment. As in the experiments, K_{slow} mainly activates during the

imposed spike train, which in the model produces a sharp rise in c (Fig. 6, A and B). During each simulated burst command, c_{ER} rises slightly during the pulse train and then recovers during the holding period as Ca^{2+} drains from the ER (Fig. 6 F). When the SERCA pump is blocked, the rise in c during the pulse train is exaggerated because all of the Ca^{2+} that enters the cell remains in the cytosol without being diverted to the ER. Consequently, the amount of K_{slow} activated by a simulated burst command increases and remains elevated as the ER store is depleted (Fig. 6, C and D). However, this prediction does not agree with the experimental data (Figs. 3 and 4), which show only a transient increase in K_{slow} after SERCA inhibition followed by current suppression. In summary, a model consisting of only the ER and cytosolic compartments, and with K_{slow} depending exclusively on c, failed to account for the transient rise and fall in K_{slow} observed experimentally.

This compelled us to include additional features in this minimal model. Following suggestions raised in other cell types (Jafri et al., 1998; Liu et al., 1998; Frieden and Graier, 2000), we hypothesized that K_{slow} could be dependent on Ca^{2+} released from the ER, as has been suggested previously for an apamin-insensitive K_{Ca} current in β-cells (Ämmala et al., 1991). Specifically, we postulate that K_{slow} channels are located in intimate proximity to ER Ca^{2+} efflux channels (Model II). Although there is no direct evidence that β-cells have the morphologic specializations of cells such as cardiac myocytes, where L-type Ca^{2+} channels are colocalized with RyR channels (Carl et al., 1995; Bers and Perez-Reyes, 1999) our modeling suggests that it is merely necessary for a portion of the ER to lie close to plasma membrane regions containing K_{slow} channels to account for our data. The presence of a subspace created by this juxtaposition would generate a local Ca^{2+} concentration gradient as long as there is a maintained Ca^{2+} flux from the ER into the subspace. Given such an arrangement, it follows that depletion of the ER would necessarily reduce K_{slow} current by eliminating the gradient; in this case, c_{SS} would fall to the level of c. If we further assume that the activation curve of K_{slow} is steeply dependent on $[Ca^{2+}]$ and that the binding constant (K_d) of K_{slow} for Ca^{2+} is significantly higher than basal levels of c, then K_{slow} current would be significantly depressed after ER store depletion. This would be expected to occur on the time scale of ER depletion after SERCA inhibition. Data from permeabilized cells indicate that the ER in β-cells empties over several minutes, comparable to the times we observed for the decay of K_{slow} after either thapsigargin or insulin application (Tengholm et al., 1998, 2000, 2001). Whether K_{slow} is nearly abolished or merely reduced depends on the affinity of K_{slow} for Ca^{2+}, and on the chosen flux parameters, which determine the magnitude of the Ca^{2+} concentration gradient between the subspace and the cytosol. Although we do not know the molecular identity of K_{slow}, nor its affinity for Ca^{2+}, our assumed K_d of 0.7 μM is comparable to that reported for small conductance (SK) K_{Ca} channels, which have been theorized to mediate the K_{slow} current (Hirschberg et al., 1998).

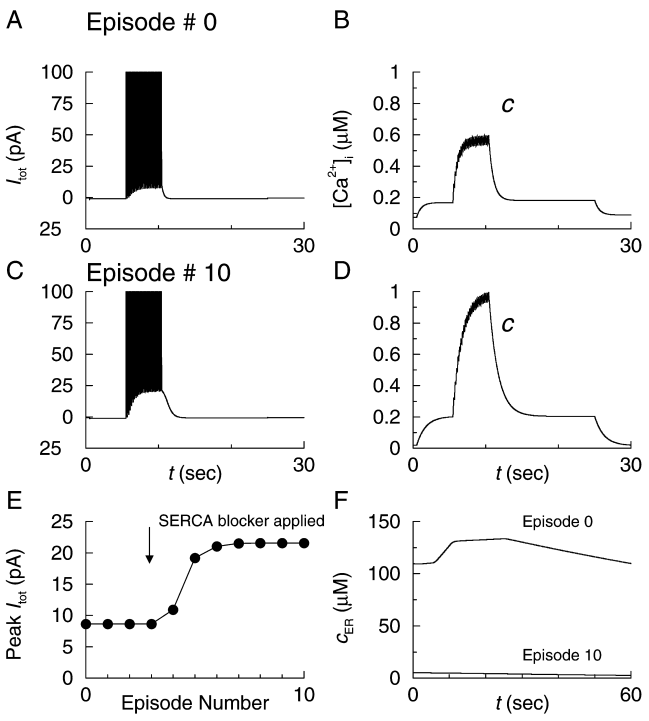

FIGURE 6. Simulation of voltage-clamp data using Model I (Eqs. 1–5). Voltage is imposed as in Fig. 2; each episode is 60 s in duration, but only the first 30 s are shown for clarity. (A and B) Total ionic current (I_{tot}) and bulk cytosolic $[Ca^{2+}]$ (c) for Episode # 0, corresponding to control conditions before SERCA pump is blocked. (C and D) Total ionic current (I_{tot}) and c for Episode # 10, corresponding to the steady-state after SERCA blockade (blocker was applied at the beginning of Episode # 3). K_{slow} is increased, not decreased, as found in the experiments with Tg (Fig. 3) and insulin (Fig. 4). (E) Peak ionic current (generally the current immediately after termination of the spike train) obtained in each episode. (F) ER $[Ca^{2+}]$ (c_{ER}) versus time for the first and last episodes, showing the depletion of the ER after SERCA blockade.

Not only is it clear that Model II can account for the loss of K_{slow} over a period of minutes following SERCA block, but this model can also reproduce the transient increase in K_{slow} observed in the first few minutes following SERCA blockade (Fig. 7 G). As shown in Fig. 7, A and B, before the block of SERCA (Episode # 0), K_{slow} develops in seconds during the pulse train and decays in seconds afterwards, as in the simpler model lacking a subspace (Model I; Fig. 6, A and B). In the subspace model, however, K_{slow} is activated by c_{SS}, not c. The subspace Ca^{2+} concentration, c_{SS}, has two components, a fast component that tracks the rapid changes in c and a nearly constant component that reflects the contribution of c_{ER}. Therefore, the rapid rise in K_{slow} observed

during the spike train mainly reflects the rapid rise in c due to Ca^{2+} entry.

It may seem paradoxical that c_{SS}, which is fed by Ca^{2+} released from the ER, can rise when c_{ER} is essentially constant. However, examination of Eqs. 8 and 10 (MATERIALS AND METHODS) reveals that a rise in c will diminish the gradient for Ca^{2+} efflux from the subspace into the bulk cytosol. Like a bathtub with a constant inflow, partially blocking the drain will cause the subspace to fill.

The dependence of c_{SS} on c and c_{ER} can be made more precise. Because the fluxes in and out of the subspace are large, the subspace is always nearly in equilibrium with the ER and the cytosol. Setting Eq. 8 to equilibrium and substituting the formulas for the fluxes (Eqs. 9 and 10), we obtain the following useful relation:

$$c_{SS} = (V_{ER}p_{ER}c_{ER} + V_{CYT}p_X c)/(V_{ER}p_{ER} + V_{CYT}p_X). \quad (11)$$

That is, one can approximate c_{SS} by a weighted average of c_{ER} and c, with the weights determined by the volumes of the ER and cytosol and the exchange rates between those compartments and the subspace.

After SERCA blockade, the amount of K_{slow} elicited by a simulated burst command initially rises (Episode # 4) because the fast component of c_{SS} increases due to the increase in c. The increase in c results from the loss of the SERCA pump, exactly as in Model I. The reason K_{slow} rises before it falls is that c_{ER} declines very slowly after SERCA is blocked. This creates a window of time in which the rise in c due to Tg has not yet been compensated for by the fall in c_{ER} that ultimately results. Thus, only after several minutes does the gradient between the subspace and the cytosol collapse, decreasing c_{SS} to the level of c. By Episode # 10 (Fig. 7, E and F), the gradient between c_{SS} and c and hence K_{slow}, are nearly abolished. Even though the change in c during the simulated burst command is larger after store depletion than before, c_{SS} remains below threshold for activation of K_{slow}. Our assumption that K_{slow} has a steep dependence on Ca^{2+} is critical for this to occur. Recall that some of our cells exhibited only inhibition, with no prior potentiation of K_{slow} after SERCA blockade. This can be accounted for in the model by quantitative variation of parameters, for example, reducing the pump rate k_{PMCA} by 1/4.

The Role of K_{slow} in Islet Bursting

Thus far, the modeling results allow us to say that a minimal implementation of the subspace idea qualitatively accounts for the experimental data we observed, whereas a simpler model consisting of only the ER and the cytosol is insufficient. The model also suggests a possible role of K_{slow} in β-cell electrical activity. Göpel et al. (1999) proposed a model based on the properties of K_{slow} deactivation after the pulse train of the simulated burst protocol. However, the subspace model suggests that the kinetics of K_{slow} activation and deactivation mainly reflect only the fast dynamics of c. We will show below (Fig. 9) that this fast component of K_{slow} is not sufficient to make K_{slow} a pacemaker for bursts lasting longer than a few seconds, whereas we and others observe burst periods ranging up to tens of seconds or minutes in situ.

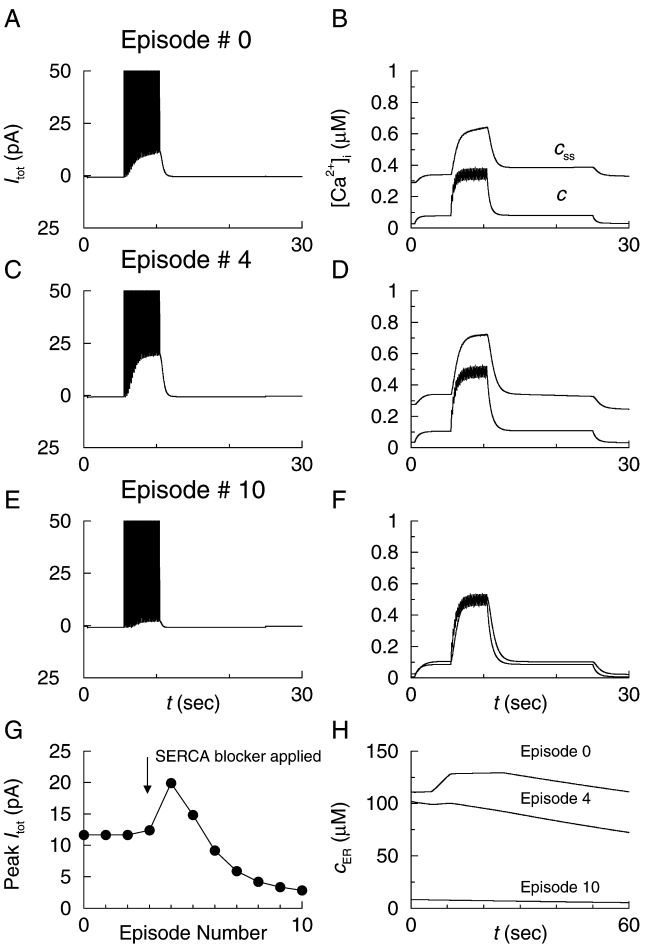

FIGURE 7. Simulation of voltage-clamp data using Model II (Eqs. 1, 2, and 6–10). Voltage protocol as in Figs. 2 and 6. Only the first 30 s of each 60 s episode are shown for clarity. (A and B) Total ionic current (I_{tot}), bulk cytosolic $[Ca^{2+}]$ (c), and subspace $[Ca^{2+}]$ (c_{SS}) for Episode # 0, corresponding to control conditions before SERCA blockade. The fast rise in c_{SS} reflects the fast rise in c due to Ca^{2+} entry. (C and D) Total ionic current (I_{tot}) and c, c_{SS} during Episode # 4, beginning 2 min after SERCA blockade. The fast rise in c_{SS} is larger than in control because of the larger rise in c. (E and F) Total ionic current (I_{tot}) and c, c_{SS} during Episode # 10, representing near steady-state conditions after SERCA blockade. The differential between c_{SS} and c has collapsed because of ER depletion (see H), leading to loss of K_{slow}. (G) Peak ionic current obtained in each episode. (H) ER $[Ca^{2+}]$ (c_{ER}) versus time for the zeroth, fourth, and tenth episodes, showing the depletion of the ER after SERCA blockade.

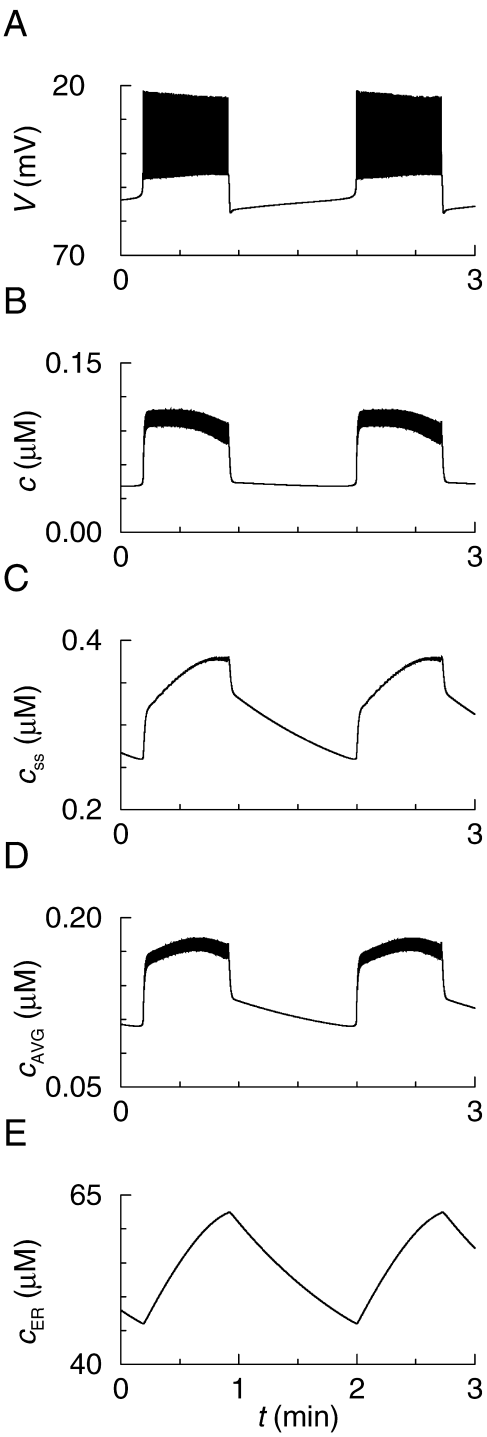

FIGURE 8. Simulation of bursting using Model II (Eqs. 1, 2, and 6–10) (voltage not clamped), showing the four dependent variables, membrane potential (V), bulk cytosolic [Ca^{2+}] (c), subspace [Ca^{2+}] (c_{SS}), and ER [Ca^{2+}] (c_{ER}). In addition, c_{AVG}, the volume-weighted average of c and c_{SS}, is shown as an approximation of what would be reported by a fluorescent dye. Note the relatively flat level of c_{AVG} during the active phase of each burst and the slow tail of decline during the silent phase. Further, c_{AVG} exhibits a decline toward the end of the active phase at the same time that the component of [Ca^{2+}] that controls K_{slow}, c_{SS}, is rising. Parameters as in Fig. 7 except: k_{PMCA} reduced from 0.18 ms^{-1} to 0.12 ms^{-1} and p_{ER} increased from 0.0015 ms^{-1} to 0.0030 ms^{-1}.

However, if K_{slow} responds to c_{SS}, which is essentially a weighted average of c and c_{ER} (compare Eq. 11), then the ER will impart a very slow component to K_{slow}. This is illustrated in Fig. 8, where we simulate bursting with the same model used for the voltage-clamp simulation shown in Fig. 7 (see the legend of Fig. 8 for minor parameter changes). The fast and slow components of K_{slow} reflect the fast and slow components in c_{SS} (Fig. 8 C). Thus, at the beginning of each active phase, c_{SS} jumps up rapidly, but the corresponding rise in K_{slow} that follows is not sufficient to terminate the burst. The maintained depolarization produces a slow rise in c_{ER} (Fig. 8 E), which is reflected in a progressive slow increase in c_{SS}. In the model, it is this slow rise in c_{SS}, and hence K_{slow}, that ultimately repolarizes the burst. A mirror image sequence occurs in the silent phase, where an initial rapid drop in c_{SS} is followed by a slow decaying phase that over many seconds removes enough K_{slow} to permit a new phase of depolarization. In addition to the concentrations of Ca^{2+} in all three compartments, Fig. 8 D shows c_{AVG}, the average of c and c_{SS} weighted by the cytosol and subspace volumes, since this would be expected to more closely correspond to the Ca^{2+} level that would actually be measured experimentally using Ca^{2+}-sensitive dyes. Note that c_{AVG} exhibits a fast rise and fall at the beginning of each active and silent phases, followed by a slow rise in the active phase and a slow fall in the silent phase. These features resemble data contained in several reports in the literature (Santos et al., 1991; Gilon and Henquin, 1992; Hellman et al., 1992), as well as our own unpublished observations (unpublished data). It is of interest that c_{AVG} actually starts to decline somewhat even before the end of the active phase. This highlights the need for caution in interpreting the role of $[Ca^{2+}]_i$: it may be that a component of Ca^{2+} that is not directly measured is actually driving the system. Thus, in the present model, it is subspace [Ca^{2+}] that rises monotonically to terminate the bursts, not [Ca^{2+}] in the cytosol.

The simulated bursts shown, which have a period of 1.5 min, are at the upper end of our data set. However, this period can be varied over two orders of magnitude, covering the full range of periods we and others have reported in the literature, by varying either the ER leak rate p_{ER} or other parameters (unpublished data). This may be one factor to account, at least in part, for the heterogeneous electrical activity of dispersed cells and islets reported in the literature.

Further, c_{SS}, as modeled here, transmits the slow drive originating in the ER to the plasma membrane. An immediate consequence of this is that membrane potential oscillations disappear if the ER is depleted by thapsigargin, resulting in continuous spike activity (Fig. 9). Due to the loss of K_{slow}, there is no longer any negative feedback in this case to turn off the spikes. (We re-

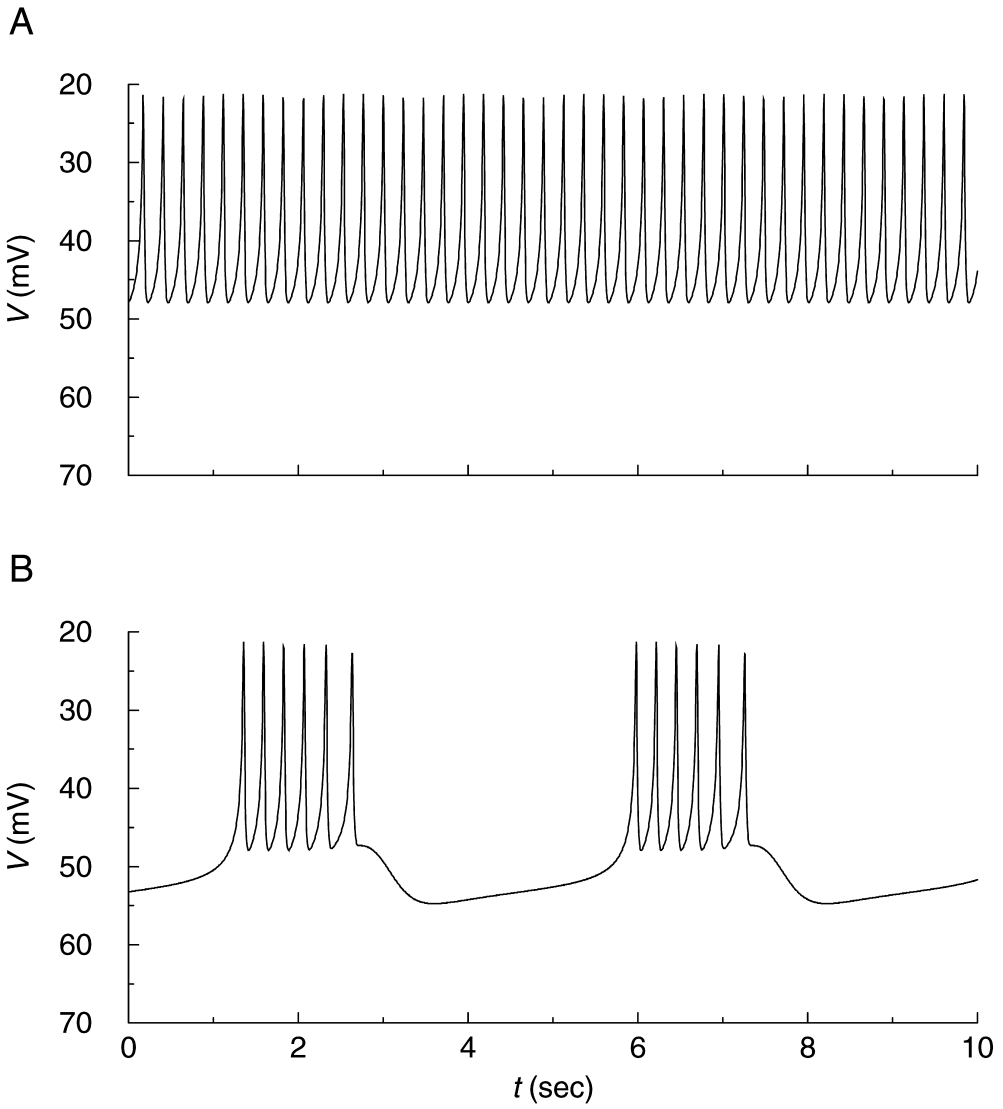

FIGURE 9. Simulation of electrical activity in the presence of thapsigargin using Model II (Eqs. 1, 2, and 6–10). (A) With SERCA blocked but all other parameters as in Fig. 8, the steady-state behavior consists of continuous spike activity because negative feedback from K_{slow} is eliminated (see Fig. 7, E and F). (B) Bursting can be restored by increasing the affinity of K_{slow} for Ca^{2+} (K_d is reduced from 0.7 to 0.2 μM), but the period is very short, only a few seconds. This is due to the fact that medium and slow bursting (Fig. 8) require the participation of the ER in this model.

strict the SERCA blocker in this simulation to be thapsigargin, and not insulin, to avoid the complication that insulin also opens $K_{[ATP]}$ channels [Khan et al., 2001]). Thus, the subspace model offers an alternative theory to the activation of CRAC or CRAN channels after store depletion of Ca^{2+}(Worley et al., 1994a,b; Roe et al., 1998; Satin and Kinard, 1998), which has been proposed to account for Tg-induced β-cell depolarization and continuous spiking (Worley et al., 1994a; Bertram et al., 1995; Gilon et al., 1999). That is, it may be the loss of outward K_{slow} current associated with Tg, rather than the activation of an inward CRAC current, that is responsible for β-cell depolarization.

It is no surprise that without negative feedback there is no bursting. However, even if the K_d of K_{slow} for Ca^{2+} is reduced in the model, so that the channel now opens at the lower c_{SS} levels that prevail after store depletion, only fast bursting is supported (Fig. 9 B). This underscores the point that in the subspace model, the slow drive in β-cell electrical oscillations stems from the ER; the faster kinetics of cytosolic Ca^{2+}, reflected in the K_{slow} tail, can produce bursts on a time scale of at most a few seconds. This suggests that the slow dynamics of ER Ca^{2+} coupled to K_{slow} through a restricted subspace may be essential for the production of 10–60 s long oscillations seen in classic in vitro islet bursts.

DISCUSSION

Two K_{Ca} channels are known to be present in β-cells: a "fast," large conductance K_{Ca}, which is strongly voltage dependent and selectively blocked by charybdotoxin (Kukuljan et al., 1991), and a slowly activating and deactivating K_{Ca} current, K_{slow}, which is relatively voltage independent and as yet has no selective blocker (Göpel et al., 1999). It has been proposed that K_{slow} is responsible for islet pacemaking and that its activation and deactivation kinetics strongly correlate with islet electrical activity (Göpel et al., 1999). It has further been hypothesized that the slower electrical behavior sometimes observed

in dispersed β-cells (Larsson et al., 1996) compared with in situ β-cells results from their having less K_{slow} current (Göpel et al., 1999). In our hands, K_{slow} current amplitude in dispersed β-cells was not vastly different from that of in situ β-cells on a cell to cell basis, despite their heterogeneous electrical activity (Kinard et al., 1999). In fact, we observed more variability in K_{slow} amplitude from cell to cell than between the two groups of cells. Thus, we conclude that differences in K_{slow} current amplitude are not sufficient to explain the differences observed in the electrical behavior of dispersed versus in situ β-cells, which remains an open question.

In the present study, we demonstrated that K_{slow} was modulated by either thapsigargin or insulin. Exposing cells to either agent resulted in an initial potentiation of K_{slow} amplitude, followed by a nearly complete and sustained suppression. The observation that insulin and thapsigargin had nearly identical effects on K_{slow} means that it is likely that both agents act on the channel secondary to SERCA inhibition and ER Ca^{2+} depletion (Thastrup et al., 1990; Islam et al., 1992; Xu et al., 1999). These data are consistent with the hypothesis that an essential component of the Ca^{2+} that activates K_{slow} channels during a burst of action potentials is provided by Ca^{2+} from ER stores and maintained SERCA activity.

We developed a mathematical model to quantitatively test this hypothesis. In this model, Ca^{2+} entering the cytosol during a burst of action potentials is pumped into the ER by SERCA. Ca^{2+} then tunnels through the organelle (Petersen et al., 2001) and exits via ER Ca^{2+} channels in a region of the cytosol that is in close proximity to plasmalemmal K_{slow} channels. The focal source of Ca^{2+} leaving the ER would provide a local gradient of $[Ca^{2+}]_i$ between the subspace and the rest of the cytosol. We further postulated that the elevated Ca^{2+} in this subspace is adequate to activate K_{slow} channels, whereas bulk cytosolic Ca^{2+} is not. For simplicity, we have modeled this condition with two discrete compartments, but we conjecture that a sufficient gradient and comparable results could be obtained using a model of continuous, buffered diffusion between the Ca^{2+} release zone and the bulk cytosol, without the need for specialized structures to hinder diffusion.

According to this model, the initial potentiation of K_{slow} after inhibition of SERCA results from a rise in c that in turn reduces Ca^{2+} efflux from the subspace and increases c_{SS}. c rises because all the Ca^{2+} ions that enter the cell through voltage-gated Ca^{2+} channels are now free to contribute to c rather than splitting their effects between the ER and the cytosolic compartments. However, because the ER contribution is critical for the activation of K_{slow} in this model, as the ER empties, the response of K_{slow} to an imposed pulse train progressively declines. This scenario requires a steeply nonlinear dependence of K_{slow} on Ca^{2+}, such that an increment of $[Ca^{2+}]_i$ on top of a super-threshold level of $[Ca^{2+}]_{SS}$ can increase the current, whereas the same increment is ineffective once the ER component is abolished.

Although this model involves a number of assumptions, we find the hypothesis appealing because we could not account for the biphasic effects of SERCA blockade with any simpler model. In Fig. 6, we show explicitly that a model incorporating only two Ca^{2+} compartments, the cytosol and the ER, could account for the rise in K_{slow} but not the fall. An alternative explanation would be to assume that both Tg and insulin have direct bi-directional effects on the channel, but this seems highly unlikely for two agents that are so structurally dissimilar.

We also considered an alternative hypothesis. In this hypothesis, store depletion activates a calcium release–activated current (CRAC/CRAN) (Worley et al., 1994a,b) that raises c sufficiently to maximally activate K_{slow} even under basal conditions. No additional K_{slow} conductance could then be elicited by the burst protocol. We rejected this model, however, because it predicts a significant increase in the size of the holding current at −65 mV, which was not observed. The hypothesis also predicts an increase in the total current elicited by stepping the command potential from −65 to −40 mV following store depletion. We did not see such an increase in cells that exhibited a loss of K_{slow} with Tg. Nor did we observe an increase in total current upon stepping from −40 to 0 mV under steady-state conditions in Tg, as would be expected if K_{slow} were maximally activated by Ca^{2+} entry through CRAC channels (Figs. 3 and 4).

Several previous studies support the hypothesis that K^+ channels can be activated by localized Ca^{2+} in a submembrane space controlled by ER calcium efflux (Berridge, 1998; Bootman et al., 2001). First, it has been shown that during the active phase of glucose-stimulated oscillations, rises in $[Ca]_i$ are buffered by Ca^{2+} uptake into the ER (Gilon et al., 1999). The passive leak of Ca^{2+} from the ER during the subsequent silent phase contributes to the slow decay in cytosolic $[Ca^{2+}]$ that is observed. Second, it has been directly demonstrated that glucose stimulation induces microgradients of Ca^{2+} localized just beneath the plasma membrane of the β-cell (Martín et al., 1997; Quesada et al., 2000). Lastly, similar mechanisms of ER-dependent activation of K_{Ca} channels have been reported in other systems. Thus, histamine-induced activation of BK K_{Ca} channels in a human umbilical vein endothelial cell line was shown to depend upon ryanodine-sensitive calcium release from intracellular Ca^{2+} stores (Frieden and Graier, 2000), and Ca^{2+}-induced Ca^{2+} release has been reported to trigger the activation of the K_{Ca} channels that mediate the after hyper-

polarizations of nodose neurons (Cordoba-Rodriguez et al., 1999).

In addition to being regulated by insulin and Tg, K_{slow} was sensitive to changes in extracellular glucose concentration. This contrasts with the reports by Göpel et al. (1999, 2001) that changes in [glucose] altered the kinetics but not the amplitude of K_{slow}. In our hands, increasing glucose from 5 to 10 mM decreased K_{slow} current density in dispersed β-cells by ~50%. Thus, in addition to K_{ATP} channels, K_{slow} may be metabolically regulated in β-cells (Cook and Hales, 1984; Rorsman and Trube, 1985).

We also used our mathematical model to explore the consequences of the subspace hypothesis for the production of islet electrical activity. We found that the slow kinetic component imparted by ER Ca^{2+} allows K_{slow} to drive oscillations with periods up to minutes in duration (Fig. 8). The period of this bursting can be reduced to tens of seconds or seconds by increasing the ER leak rate, decreasing K-ATP conductance, or varying other parameters (unpublished data). Thus, the model can reproduce the full range of bursting time scales observed experimentally. This dynamic flexibility stems from the interaction of two slow negative feedback processes, c and c_{ER}, with time scales of a few seconds and a few minutes, respectively, which can mix to produce a range of intermediate time scales. Thus, the subspace model is an exemplar of the general class of models we call "phantom bursters" (Bertram et al., 2000).

In contrast, with the ER inhibited, burst period is limited to at most a few seconds (Fig. 9, bottom), unless the PMCA pump rate is reduced to make the kinetics of cytosolic Ca^{2+} much slower than what we observe (unpublished data). Note that some previous models (Chay, 1996, 1997) also exhibit a wide range of burst periods based on the interaction of cytosol and ER compartments. However, since these models lack a Ca^{2+} subspace, they fail to account for the effects of SERCA blockade on K_{slow}.

The behavior of the subspace model is also compatible with experiments in which modulation of β-cell ER Ca^{2+} stores influences islet electrical activity and insulin secretion. Thus, the exposure of mouse islets to 1–5 μM Tg has been shown to disrupt regular bursting, leading to sustained depolarization, continuous spiking and increased glucose-induced insulin secretion (Worley et al., 1994a,b; Bertram et al., 1995; Gilon et al., 1999). These findings have been interpreted previously to reflect the activation of a store-dependent depolarizing current, CRAC. However, as shown in the present study, depleting ER Ca^{2+} stores by SERCA pump blockade could alternatively result in islet depolarization via K_{slow} inhibition. On the other hand, an additional inward current such as CRAC/CRAN may still be required to explain depolarization following activation of ER efflux, which does not inhibit K_{slow} in the subspace model (unpublished data).

In summary, the model proposed here sheds new light on the potential role of K_{Ca} channels in islet pacemaking, a role that we suggest can only be fully realized in partnership with ER Ca^{2+} stores and a submembrane compartment. Because K_{slow} activation is dependent on the ER and regulated by agents that alter ER Ca^{2+}, these agents may provide novel tools to further investigate the role of K_{Ca} channels and intracellular Ca^{2+} stores in the electrical activity of β-cells. While we have focused on K_{slow} in this paper, we believe that there may well be other important slow negative feedback mechanisms involved in β-cell pacemaking. These include inactivation of Ca^{2+} channels or activation of K_{ATP} channels due to depolarization, Ca^{2+} entry, and/or insulin secretion (Cook et al., 1991). Further work will be needed to dissect the rhythmogenic roles played by these complementary mechanisms.

We thank Heather Strange for preparing the cell cultures. Modeling was done by A. Sherman and R. Bertram and experiments were done by P. Goforth, M. Zhang, F. Khan, and L.S. Satin.

This work was partially supported by National Science Foundation grants DMS-9981822 and DBI-9602233 to R. Bertram and National Institutes of Health grant RO1 DK-46409 to L. Satin.

Submitted: 20 February 2002
Revised: 24 May 2002
Accepted: 5 June 2002

REFERENCES

Ämmala, C., O. Larsson, P.O. Berggren, K. Bokvist, L. Juntti-Berggren, H. Kindmark, and P. Rorsman. 1991. Inositol trisphosphate-dependent periodic activation of a Ca(2+)-activated K+ conductance in glucose-stimulated pancreatic beta-cells. *Nature.* 353:849–852.

Arredouani, A., J.C. Henquin, and P. Gilon. 2002. Contribution of the endoplasmic reticulum to the glucose-induced $[Ca^{2+}]_c$ response in mouse pancreatic islets. *Am. J. Physiol. Endocrinol. Metab.* 282:982–991.

Ashcroft, F.M., and P. Rorsman. 1989. Electrophysiology of the pancreatic β-cell. *Prog. Biophys. Mol. Biol.* 54:87–143.

Atwater, I., C.M. Dawson, B. Ribalet, and E. Rojas. 1979. Potassium permeability activated by intracellular calcium ion concentration in the pancreatic β-cell. *J. Physiol.* 288:575–588.

Aulbach, F., A. Simm, S. Maier, H. Langenfeld, U. Walter, U. Kersting, and M. Kirstein. 1999. Insulin stimulates the L-type Ca^{2+} current in rat cardiac myocytes. *Cardiovasc. Res.* 44:390–397.

Barker, C.J., T. Nilsson, C.J. Kirk, R.H. Michell, and P.O. Berggren. 1994. Simultaneous oscillations of cytoplasmic free Ca^{2+} concentration and Ins(1,4,5)P3 concentration in mouse pancreatic beta-cells. *Biochem. J.* 297:265–268.

Berridge, M.J. 1998. Neuronal calcium signaling. *Neuron.* 21:13–26.

Bers, D.M., and E. Perez-Reyes. 1999. Ca channels in cardiac myocytes: structure and function in Ca influx and intracellular Ca release. *Cardiovasc. Res.* 42:339–360.

Bertram, R., P. Smolen, A. Sherman, D. Mears, I. Atwater, F. Martin, and B. Soria. 1995. A role for calcium-release activated current (CRAC) in cholinergic modulation of electrical activity in pancreatic β-cells. *Biophys. J.* 68:23223–23232.

Bertram, R., J. Previte, A. Sherman, T.A. Kinard, and L.S. Satin. 2000. The phantom burster model for pancreatic β-cells. *Biophys. J.* 79:2880–2892.

Bootman, M.D., P. Lipp, and M.J. Berridge. 2001. The organisation and functions of local Ca^{2+} signals. *J. Cell Sci.* 114:2213–2222.

Carl, S.L., K. Felix, A.H. Caswell, N.R. Brandt, W.J. Ball, Jr., P.L. Vahgy, G. Meissner, and D.G. Ferguson. 1995. Immunolocalization of sarcolemmal dihydropyridine receptor and sarcoplasmic reticular triadin and ryanodine receptor in rabbit ventricle and atrium. *J. Cell Biol.* 129:672–682.

Chay, T.R. 1996. Electrical bursting and luminal calcium oscillation in excitable cell models. *Biol. Cybern.* 75:419–431.

Chay, T.R. 1997. Effects of extracellular calcium on electrical bursting and intracellular and luminal calcium oscillations in insulin secreting pancreatic β-cells. *Biophys. J.* 73:1673–1688.

Chay, T.R., and J. Keizer. 1985. Minimal model for membrane oscillations in the pancreatic β-cell. *Biophys. J.* 42:181–190.

Cook, D.L. 1984. Electrical pacemaker mechanisms of pancreatic islet cells. *Fed. Proc.* 43:2368–2372.

Cook, D.L., and C.N. Hales. 1984. Intracellular ATP directly blocks K^+ channels in pancreatic β-cells. *Nature.* 311:271–273.

Cook, D.L., M. Ikeuchi, and W. Fujimoto. 1984. Voltage-dependence of rhythmic plateau potentials of pancreatic islet cells. *Am. J. Physiol.* 240:E290–E296.

Cook, D.L., L.S. Satin, and W.F. Hopkins. 1991. Pancreatic β cells are bursting, but how? *Trends Neurosci.* 14:411–414.

Cordoba-Rodriguez, R., K.A. Moore, J.P. Kao, and D. Weinreich. 1999. Calcium regulation of a slow post-spike hyperpolarization in vagal afferent neurons. *Proc. Natl. Acad. Sci. USA.* 96:7650–7657.

Dean, P.M., and E.K. Matthews. 1968. Electrical activity in pancreatic islet cells. *Nature.* 219:389–390.

Dean, P.M., and E.K. Matthews. 1970. Electrical activity of pancreatic islet cells: effect of ions. *J. Physiol.* 210:265–275.

Falke, L.C., K.D. Gillis, D.M. Pressel, and S. Misler. 1989. 'Perforated patch recording' allows long-term monitoring of metabolite-induced electrical activity and voltage-dependent Ca^{2+} currents in pancreatic islet β cells. *FEBS Lett.* 251:167–172.

Frieden, M., and W.F. Graier. 2000. Subplasmalemmal ryanodine-sensitive Ca^{2+} release contributes to Ca^{2+}-dependent K^+ channel activation in human umbilical vein endothelial cell line. *J. Physiol.* 524:715–724.

Gilon, P., A. Arredouani, P. Gailly, J. Gromada, and J.C. Henquin. 1999. Uptake and release of Ca^{2+} by the endoplasmic reticulum contribute to the oscillations of the cytosolic Ca^{2+} concentration triggered by Ca^{2+} influx in the electrically excitable pancreatic β-cell. *J. Biol. Chem.* 274:20197–20205.

Gilon, P., and J.C. Henquin. 1992. Influence of membrane potential changes on cytoplasmic Ca^{2+} concentration in an electrically excitable cell, the insulin-secreting pancreatic β-cell. *J. Biol. Chem.* 267:20713–20720.

Göpel, S.O., T. Kanno, S. Barg, L. Eliasson, J. Galvanovskis, E. Renström, and P. Rorsman. 1999. Activation of Ca^{2+}-dependent K^+ channels contributes to rhythmic firing of action potentials in mouse pancreatic β-cells. *J. Gen. Physiol.* 114:759–769.

Göpel, S.O., T. Kanno, and P. Rorsman. 2001. Two components of activity-dependent transient K^+-current (I_{Kslow}) in mouse pancreatic β-cells. *Diabetologia.* 44:A20.

Gromada, J., J. Frokjaer-Jensen, and S. Dissing. 1996. Glucose stimulates voltage- and calcium-dependent inositol trisphosphate production and intracellular calcium mobilization in insulin-secreting beta TC3 cells. *Biochem. J.* 314:339–345.

Hellman, B., E. Gylfe, E. Grapengiesser, P.E. Lund, and A. Berts. 1992. Cytoplasmic Ca^{2+} oscillations in pancreatic β-cells. *Biochem. et Biophys. Acta.* 1113:295–305.

Hennige, A.M., N. Lembert, M.A. Wahl, and H.P. Ammo. 2000. Oxidative stress increases potassium efflux from pancreatic islets by depletion of intracellular calcium stores. *Free Radic. Res.* 33:507–516.

Herrington, J., and R.J. Bookman. 1994. Pulse Control v4.3 Igor XOPs for Patch Clamp Data Acquisition. University of Miami Press, Miami, FL.

Hirschberg, B., J. Maylie, J.P. Adelman, and N.V. Marrion. 1998. Gating of recombinant small conductance Ca-activated K+ channels by calcium. *J. Gen. Physiol.* 111:565–581.

Islam, M.S., I. Leibiger, B. Leibiger, D. Rossi, V. Sorrentino, T.J. Ekstrom, H. Westerblad, F.H. Andrade, and P.O. Berggren. 1998. In situ activation of the type 2 ryanodine receptor in pancreatic beta cells requires cAMP-dependent phosphorylation. *Proc. Natl. Acad. Sci. USA.* 95:6145–6150.

Islam, M.S., P. Rorsman, and P.O. Berggren. 1992. Ca^{2+}-induced Ca^{2+} release in insulin-secreting cells. *FEBS Lett.* 296:287–291.

Jafri, M.S., J.J. Rice, and R.L. Winslow. 1998. Cardiac Ca^{2+} dynamics: the roles of ryanodine receptor adaptation and sarcoplasmic reticulum load. *Biophys. J.* 74:1149–1168.

Khan, F.A., P.B. Goforth, M. Zhang, and L.S. Satin. 2001. Insulin activates ATP-sensitive K^+ channels in pancreatic β-cells through a phosphatidylinositol 3-kinase-dependent pathway. *Diabetes.* 50: 2192–2198.

Kinard, T.A., G. de Vries, A. Sherman, and L.S. Satin. 1999. Modulation of the bursting properties of single mouse pancreatic beta cells by artificial conductances. *Biophys. J.* 76:1423–1435.

Kozak, J.A., S. Misler, and D.E. Logothetis. 1998. Characterization of a Ca2+-activated K+ current in insulin-secreting murine beta TC-3 cells. *J. Physiol.* 509:355–370.

Kukuljan, M., A.A. Goncalves, and I. Atwater. 1991. Charybdotoxin-sensitive Kca channel is not involved in glucose-induced electrical activity in pancreatic β-cells. *J. Membr. Biol.* 119:187–195.

Larsson, O., H. Kindmark, R. Branstrom, B. Fredholm, and P.O. Berggren. 1996. Oscillations in K_{ATP} channel activity promote oscillations in cytoplasmic free Ca^{2+} concentration in the pancreatic β-cell. *Proc. Natl. Acad. Sci. USA.* 93:5161–5165.

Liu, Y.J., E. Grapengiesser, E. Gylfe, and B. Hellman. 1995. Glucose induces oscillations of cytoplasmic Ca^{2+}, Sr^{2+}, and Ba^{2+}, in pancreatic β-cells without participation of the thapsigargin-sensitive store. *Cell Calcium.* 18:165–173.

Liu, Y.J., E. Grapengiesser, E. Gylfe, and B. Hellman. 1996. Crosstalk between the cAMP and inositol trisphosphate-signaling pathways in pancreatic beta-cells. *Arch. Biochem. Biophys.* 334:295–302.

Liu, Y.J., and E. Gylfe. 1997. Store-operated Ca^{2+} entry in insulin-releasing pancreatic beta-cells. *Cell Calcium.* 22:277–286.

Liu, X., E. Rojas, and I.S. Ambukar. 1998. Regulation of KCa current by store-operated Ca^{2+} influx depends on internal Ca^{2+} release in HSG cells. *Am. J. Physiol.* 275:C571–C580.

Martín, F., J. Ribas, and B. Soria. 1997. Cytosolic Ca^{2+} gradients in pancreatic islet cells stimulated by glucose and carbachol. *Biochem. Biophys. Res. Commun.* 235:465–468.

Meissner, H.P., and H. Schmelz. 1974. Membrane potential of beta-cells in pancreatic islets. *Pflugers Arch.* 351:195–206.

Meissner, H.P., and W. Schmeer. 1981. The significance of calcium ions for the glucose-induced electrical activity of pancreatic β-cells. *In* The Mechanism of Gated Calcium Transport Across Biological Membranes. S. Ohnishi and M. Endo, editors. Academic Press, New York, NY. 324 pp.

Miura, Y., J.C. Henquin, and P. Gilon. 1997. Emptying of intracellular Ca^{2+} stores stimulates Ca^{2+} entry in mouse pancreatic β-cells by both direct and indirect mechanisms. *J. Physiol.* 503:387–398.

Petersen, O.H., A. Tepikin, and M.K. Park. 2001. The endoplasmic reticulum: one continuous or several separate Ca^{2+} stores? *Trends*

Neurosci. 24(5):271–276.

Quesada, I., F. Martín, and B. Soria. 2000. Nutrient modulation of polarized and sustained submembrane Ca^{2+} microgradients in mouse pancreatic islet cells. *J. Physiol.* 525:159–167.

Ribalet, B., and P.M. Beigelman. 1981. Effects of divalent cations on β-cell electrical activity. *Am. J. Physiol.* 241:C59–C67.

Roe, M.W., J.F. Worley III, F. Qian, N. Tamarina, A.A. Mittal, F. Dralyuk, N.T. Blair, R.J. Mertz, L.H. Philipson, and I.D. Dukes. 1998. Characterization of a Ca^{2+} release-activated nonselective cation current regulating membrane potential and $[Ca^{2+}]_I$ oscillations in transgenically derived beta-cells. *J. Biol. Chem.* 273:10402–10410.

Rorsman, P., and G. Trube. 1985. Glucose dependent K^+ channels in pancreatic beta-cells are regulated by intracellular ATP. *Pflugers Arch.* 405:305–309.

Rosario, L.M., R.M. Barbosa, C.M. Antunes, A.M. Silva, A.J. Abrunhosa, and R.M. Santos. 1993. Bursting electrical activity in pancreatic beta-cells: evidence that the channel underlying the burst is sensitive to Ca^{2+} influx through L-type Ca^{2+} channels. *Pflugers Arch.* 424:439–447.

Santos, R.M., L.M. Rosario, A. Nadal, J. Garcia-Sancho, B. Soria, and M. Valdeolmillos. 1991. Widespread synchronous $[Ca^{2+}]_i$ oscillations due to bursting electrical activity in single pancreatic islets. *Pflugers Arch.* 418:417–422.

Satin, L.S., and T.A. Kinard. 1998. Neurotransmitters and their receptors in the islets of Langerhans of the pancreas: what messages do acetylcholine, glutamate, and GABA transmit? *Endocrine.* 8:213–223.

Satin, L.S., and P.D. Smolen. 1994. Electrical bursting in β-cells of the islets of Langerhans of the pancreas. *Endocrine.* 2:677–687.

Sherman, A. 1996. Contributions of modeling to understanding stimulus-secretion coupling in pancreatic β-cells. *Am. J. Physiol.* 34:E362–E372.

Tengholm, A., C. Hagman, E. Gylfe, and B. Hellman. 1998. In situ characterization of nonmitochondrial Ca^{2+} stores in individual pancreatic β-cells. *Diabetes.* 47:1224–1230.

Tengholm, A., B. Hellman, and E. Gylfe. 2000. Mobilization of Ca^{2+} stores in individual pancreatic beta-cells permeabilized or not with digitonin or alpha-toxin. *Cell Calcium.* 27:43–51.

Tengholm, A., B. Hellman, and E. Gylfe. 2001. The endoplasmic reticulum is a glucose-modulated high-affinity sink for Ca^{2+} in mouse pancreatic beta-cells. *J. Physiol.* 530:533–540.

Thastrup, O., P.J. Cullen, B.K. Drobak, M.R. Hanley, and A.P. Dawson. 1990. Thapsigargin, a tumor promoter, discharges intracellular Ca^{2+} stores by specific inhibition of the endoplasmic reticulum Ca^{2+}-ATPase. *Proc. Natl. Acad. Sci. USA.* 87:2466–2470.

Wollheim, C.B., and W.G. Sharp. 1981. Regulation of insulin release by calcium. *Physiol. Revs.* 61:914–973.

Worley, J.F. III, M.S. McIntyre, B. Spencer, R.J. Mertz, M.W. Roe, and I.D. Dukes. 1994a. Endoplasmic reticulum calcium store depletion regulates membrane potential in mouse islet β-cells. *J. Biol. Chem.* 269:14359–14362.

Worley, J.F. III, M.S. McIntyre, B. Spencer, and I.D. Dukes. 1994b. Depletion of intracellular Ca^{2+} stores activates a maitotoxin-sensitive nonselective cationic current in beta-cells. *J. Biol. Chem.* 269:32055–32058.

Xu, G.G., Z.-Y. Gao, P.D. Borge, and B.A. Wolf. 1999. Insulin receptor substrate-1 induced inhibition of endoplasmic reticulum Ca^{2+} uptake in β-cells. *J. Biol. Chem.* 274:18067–18074.